PIER C

(Received 19 February 2025, Accepted 8 April 2025, Scheduled 31 May 2025)

Analysis of Absorbed Power Density and Power Loss Density in Human Skin Model from 5G mmWave Exposure

Ibrahim Tahir[1], Aduwati Sali[2, 3, *], Sangin Qahtan Wali[3], Alyani Ismail[3], Darko Suka[4], and Muhammad Zamir Mohyedin[2, *]

[1] *Science & Technology Research Institute for Defence (STRIDE)*
Kompleks Induk STRIDE, Taman Bukit Mewah Fasa 9, 43000 Kajang, Selangor, Malaysia
[2] *Institute for Mathematical Research (INSPEM), Universiti Putra Malaysia, 43400 Serdang, Selangor, Malaysia*
[3] *WiPNET Research Centre, Department of Computer and Communication Systems Engineering*
Faculty of Engineering, Universiti Putra Malaysia (UPM), 43400 Serdang, Selangor, Malaysia
[4] *Faculty of Electrical Engineering, University of East Sarajevo, 71123 East Sarajevo, Bosnia and Herzegovina*

ABSTRACT: This study investigates the Absorbed Power Density (APD) and Power Loss Density (PLD) of 5G downlink signals in Frequency Range 2 (FR2), in particular at millimetre-wave (mmWave) frequencies, in an outdoor scenario in Malaysia. The electric field (E-field) was measured, and the data were collected from a base station (BS) located in Cyberjaya, Malaysia, operating at 29.5 GHz, as documented in previous work of the authors. The APD and PLD were simulated using Computer Simulation Technology (CST) software. The radiation source was modelled using a patch antenna, while a four-layer human skin model represented the sample. This work simulated three different types of applications: voice calls, video calls, and video streaming. It was found that the maximum APD is 0.0364 W/m^2 for voice calls, 0.0498 W/m^2 for video calls, and 0.0584 W/m^2 for video streaming. All the investigated applications produced APD within the safe limit of 20 W/m^2 set by the International Commission on Non-Ionizing Radiation Protection (ICNIRP). PLD was analysed to investigate the depth of radiation penetration into the skin. The results show that the PLD decreased from 18.1 W/m^3 to 3.1 W/m^3, 24.8 W/m^3 to 4.1 W/m^3, and 29.1 W/m^3 to 4.8 W/m^3 from the skin surface to the skin at 1 mm depth for voice call, video call, and video streaming, respectively. It shows a significant drop in PLD due to the short wavelength of the mmWave frequencies.

1. INTRODUCTION

Malaysia is actively deploying 5G infrastructure targeting 80% coverage in populated areas nationwide by end of 2024. Additionally, Digital National Berhad (DNB) also aims to soon establish Malaysia's first standalone 5G core for the millimeter-wave (mmWave) spectrum, aligning with the country's IR 4.0 agenda and vision of Shared Prosperity by 2030 [1].

Mobile network operators struggle to meet growing demand for diversified mobile services because of limitations in the available spectrum, such as path loss and capacity. To address this demand, high frequency bands for mobile systems and wireless networks are needed. The frequency spectrum is crucial for the future advancement of 5G [2]. Frequencies which below 2 GHz are suitable for wide coverage, whereas frequencies above 3 GHz provide ample bandwidth for high data rates [3]. The former is often used for the operation of 4G long-term evolution (LTE) cellular systems, whereas the latter has more path loss, resulting in a lower coverage range [4, 5]. To meet the requirement for high coverage, data throughput, low latency, and dependability, 5G services must operate in a wide range of frequencies, i.e., Frequency Range 1 (FR1) and Frequency Range 2 (FR2). Additionally, to achieve adequate coverage, 5G must coexist with 4G LTE in low frequency bands since 4G services continue to dominate the mobile communications industry for the foreseeable future [6].

mmWave technology offers advantages such as higher data rates and very low latency compared to C-band [7]. This network is critical in supporting growing technologies and larger data usage applications. Realizing the importance of mmWave technology, it is crucial to understand its impact fully. mmWave has a shorter wavelength than other frequencies allocated for 5G and frequencies used by the previous generations. Short-range wavelengths offer advantages such as smaller device sizes, narrower beamwidth, and improved resolution. The mmWave bandwidth also allows better resilience to interference. Furthermore, it is recognized as an ideal choice for overcoming the frequency shortage in the spectrum and maximizing the use of the designated accessible frequency band [8, 9]. However, shorter wavelengths cause the coverage to be very limited, and the path loss is much higher than C-band as it is influenced by the behaviours of obstruction, diffraction, foliage loss, water absorption, and rain attenuation. Therefore, more base stations (BSs) and directed beams (beamforming) are required, which will increase human exposure to electromagnetic fields (EMFs) [10].

The growing usage of 5G technologies has prompted health concern regarding the increased radio-frequency electromagnetic field (RF-EMF) exposure among the public [11–13]. The transition to a 5G cellular system has significant adjustments,

* Corresponding authors: Muhammad Zamir Mohyedin (zamirmohyedin@upm.edu.my); Aduwati Sali (aduwati@upm.edu.my).

potentially resulting in increased RF-EMF exposure. First, the deployment of more BSs is expected due to the short wavelength and low penetration through obstacles of 5G signals. Therefore, more 5G BSs are needed to cover the same area than the number of 4G BSs since the coverage of a 5G BS is smaller than that of a 4G [14]. Namely, 5G BSs provide connectivity for smaller areas, thus being situated closer to users potentially increasing the RF-EMF exposure. Second, to achieve high data transmission rates, 5G provides higher transmission power at the receivers' side [15, 16]. As a result, users will be exposed to increased RF-EMF levels. Third, massive MIMO (mMIMO) is an expansion of MIMO (Multiple Input Multiple Output) technology that uses hundreds or even thousands of antennas connected to a BS to enhance the spectral efficiency and throughput. This technology combines antennas, radios, and spectrum to increase the capacity and speed of the 5G [17, 18]. The ability of mMIMO to improve throughput and spectrum efficiency has made it an important technology for developing wireless standards. Additionally, mMIMO in 5G improves the characteristics of the signal in terms of penetration through obstacles and enhances the coverage. In particular, 5G systems operating in C-band utilize narrow beamwidth to improve the coverage, increase directivity, and reduce the interference [19, 20]. The usage of narrow beamwidth typically employs mMIMO antennas which, as a consequence, potentially increase RF-EMF exposure causing humans to be more susceptible to it [21, 22].

A previous work from our group has measured maximum RF-EMF exposure from mmWave technology at Cyberjaya, Malaysia [23]. As shown in Figure 1, the measurement was carried out at 22 m from the BS, at a location receiving the strongest signal power. Six different tests were taken: No User Equipment (NO UE), Video Call [WhatsApp], Voice Call [WhatsApp], Video Streaming [YouTube], 100% Uplink, and 100% Downlink. The 'NO UE' test scenario represents an environment where no user equipment (UE) is actively transmitting or receiving signals. This setup allows for the measurement of ambient RF-EMF exposure solely from the base station, without interference from mobile device activity. This scenario is crucial for establishing a baseline RF-EMF exposure level. For each test, readings considered measurements at three different time intervals (1 minute, 6 minutes, and 30 minutes).

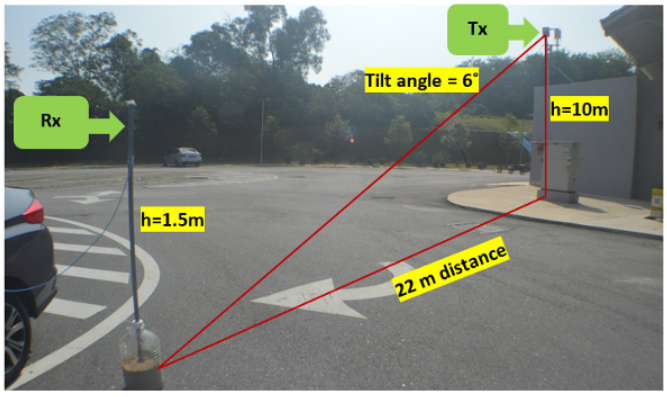

FIGURE 1. The measurement site at Cyberjaya, Malaysia [23].

The study found that video streaming produced higher RF-EMF exposure than the other tests. However, the effects of such exposure to the human body were unexplored.

Most studies so far investigated the effects of RF-EMF exposure on the human body for the frequencies in the Sub-6 GHz range [24–27]. Namely, several studies were conducted involving Specific Absorption Rate (SAR) measurements at frequencies of 900 MHz and 1800 MHz. One of them utilized a head with Cochlear implant model to investigate SAR in open and closed areas at 900 MHz and 1800 MHz. The study found that the exposure in closed areas (elevator) had a maximum SAR value of 3.5729 W/kg which is higher than the recommended SAR limit in the European standard limit. Additionally, the SAR of human head with Cochlear implant is shown to be higher from 5 to 10% than the SAR without Cochlear implant [28]. Recent report illustrates comprehensive study on the value of SAR based on age, gender, and tissue types within 900 MHz and 1800 MHz. For gender and age, it was found that adult male had the highest SAR at the head region with the value of 5.15 W/kg, followed by adult female (4.46 W/kg), child (3.67 W/kg), and baby (1.75 W/kg). Overall, $SAR_{10\,g}$ values vary based on the excitation signal strength, model type, and tissue. Furthermore, the SAR value also varies depending on the demographic group [29]. Importantly, the report claims that wireless 5G/6G devices employing mmWave frequencies, which are becoming more common in the future, have higher SAR values. Another study investigated the effects of 4G RF-EMF exposure at 1800 MHz using various antenna models. The results showed that different antennas produced different exposure effects [30]. Based on the reported review, a range of studies from 1978 to 2021 showed that SAR values from the frequencies below mmWave are considered safe [12].

The impacts of exposure to mmWave fields in terms of SAR parameter were also investigated. One study shows that SAR from 28 GHz and 38 GHz was 0.963 W/kg and 0.583 W/kg, respectively, which are safe and acceptable values [31]. Another study shows that an antipodal linear tapered slot antenna (ALTSA) operating at 60 GHz shows that the SAR values from the head and anterior thighs are below the safety levels [32]. SAR calculation and temperature response on one-layer and three-layer skin models were investigated at the frequencies of 28 GHz, 40 GHz, and 60 GHz. It was found that the SAR value at 60 GHz is higher than SAR values at 40 GHz and 28 GHz, both being equal to 0.9757 W/kg and below the safe limit. Additionally, the three-layer skin model shows higher temperature elevation than single-layer skin model [33].

Despite the lower SAR values at the mmWave frequencies, ICNIRP describes exposure above 6 GHz to 300 GHz using APD instead of SAR [34–36]. Furthermore, when higher frequencies are used, the skin depth diminishes due to the shorter wavelength, whereas the energy absorption is often restricted to the skin's surface. Studies indicate that the skin's epidermis or dermis absorbs approximately 90% of the power density at frequencies ranging from 10 GHz to 100 GHz [37]. In such cases, it is difficult to generate a significant volume for SAR. The mmWave devices operating at such high frequencies should be analyzed using power density, which is expressed per unit area

for near-field RF-EMF exposure evaluation, rather than per unit mass in SAR [34, 35].

Nevertheless, continuous reliable assessment and research on the effect of RF-EMF exposure were encouraged, even pressed to ensure a safe environment for the public. This is indicated by the development of the protocol for systematic review, frequent revision of the guidelines and needed for effective assessment technologies regarding RF's effect on human health [38–43]. Finally, this study attempts to continue previous work from our group by investigating the effects of RF-EMF exposure to mmWave by measuring absorbed power density (APD) and power loss density (PLD). Most investigations related to the effects of RF-EMF exposure on human health are limited to below 3 GHz (low-frequency) and mmWave frequencies (above 30 GHz). Therefore, this work is crucial for experimentally demonstrating the degree of radiated exposure from a 5G mmWave BS. The main contributions of the paper are:

i) Using computer simulation technology (CST) Studio Suite, an antenna was designed to represent a radiation source for the layers of the human skin model in the mmWave frequency range (29.5 GHz).

ii) APD (W/m^2) and PLD (W/m^3) from three applications (voice call, video call, and video streaming) were analyzed.

iii) This paper extends the previous work by [23]. However, in the previous work, the authors covered only the maximum RF-EMF exposure, whereas, in this paper, the effect of such exposure to the human body, specifically on skin, is investigated.

2. METHODOLOGY

To study the effects of SAR, organs or tissues were selected based on a comprehensive literature review. The skin organ was chosen after considering the characteristics of electromagnetic (EM) propagation at 29.5 GHz, also after finding a lack of research conducted using the stratified model of skin. Human skin consists of several layers; stratum corneum, epidermis and dermis, fat, and muscle. For each of these layers, relative permittivity, conductivity, thickness, and mass density data are obtained from literature [44]. Instead of SAR, the measurements were conducted in terms of APD and PLD. ICNIRP has used APD as the reference level in its guidelines for frequency above 6 GHz [34]. Meanwhile, PLD is used to simulate the depth of penetration of EMFs.

2.1. Radiation Source

A patch antenna was designed to operate at 29.5 GHz to generate the required electric field. Its directional radiation characteristics make it suitable for the exposure analysis conducted in this study. It is widely used in 5G applications due to its ability to direct energy efficiently, minimizing interference while maximizing exposure assessment accuracy [45–47]. The substrate permittivity and thickness data are based on Roger RT/Duroid 5880 substrate specifications.

A small gap of approximately 1 mm was maintained between the antenna and skin model in the simulation. By adjusting the input power, the E-field strength on the skin surface was ensured to match the values from the previous study, maintaining consistency with real-world measurements.

The following formulas summarize the antenna design process. The width W of the patch is calculated using the formula [48]:

$$W = \frac{c}{2f}\sqrt{\frac{2}{\varepsilon_r + 1}} \tag{1}$$

where c is the speed of light, f the operating frequency, and ε_r the dielectric constant of the substrate. The effective refractive index ε_{eff} is determined by [48]:

$$\varepsilon_{eff} = \frac{\varepsilon_r + 1}{2} + \frac{\varepsilon_r - 1}{2}\left[1 + 12\frac{h}{W}\right]^{-\frac{1}{2}} \tag{2}$$

where h is the height of the substrate. The effective length L_{eff} of the patch is given by [48]:

$$L_{eff} = \frac{c}{2f\sqrt{\varepsilon}_{eff}} \tag{3}$$

The length extension ΔL can be calculated as [48]:

$$\Delta L = 0.412h\frac{(\varepsilon_{eff} + 3)(\frac{W}{h} + 0.264)}{(\varepsilon_{eff} - 0.258)(\frac{W}{h} + 0.8)} \tag{4}$$

The final length L of the patch is then [48]:

$$L = L_{eff} - 2\Delta L \tag{5}$$

The dimensions of the designed antenna are indicated in Figure 2.

2.2. Human Skin Model

As illustrated in Figure 3, the designed skin model was composed of stratum corneum, epidermis and dermis, fat, and muscle. The dimensions for each layer are set at 20 mm × 20 mm, with thicknesses based on guidelines provided by ICNIRP and a literature [34, 44].

Table 1 lists the dimensions of each layer. Table 2, on the other hand, presents the permittivity, conductivity, mass density, and thickness for each tissue type that is essential for modeling the human skin as real as possible.

TABLE 1. Dimension of skin model.

Layer	Size
Stratum Corneum (SC)	20 mm × 20 mm × 0.02 mm
Viable Epidermis and Dermis	20 mm × 20 mm × 0.46 mm
Fat	20 mm × 20 mm × 1.1 mm
Muscle	20 mm × 20 mm × 30 mm

Figure 4 shows the antenna's location and orientation, with the patch oriented towards the stratum corneum layer.

TABLE 2. Properties of each tissue layer of the skin model [44].

Tissue	Permittivity	Conductivity [S/m]	Mass Density [kg/m^3]	Thickness [mm]
Stratum Corneum	3.52	1.21	1500	0.02
Viable Epidermis and Dermis	16	27.5	1109	0.46
Fat	3.42	2.32	911	1.1
Muscle	21.5	39.9	1090	∞

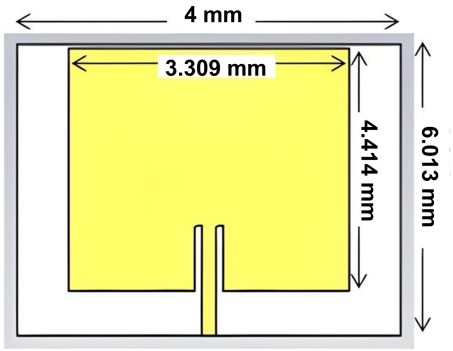

FIGURE 2. The dimensions of the designed antenna.

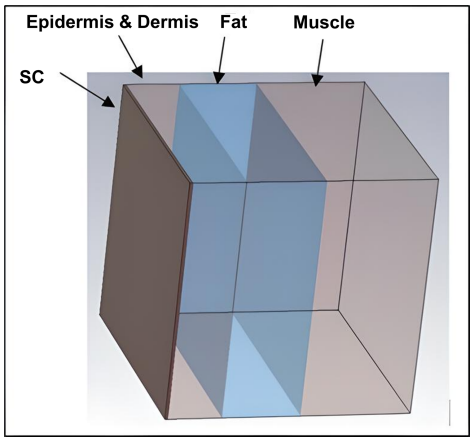

FIGURE 3. The designed skin model.

2.3. Simulation Model

To simulate the interaction between power density and skin model, EMF measurement data from Wali et al. [23] were used. These real-world measurements, conducted in Cyberjaya, Malaysia at 29.5 GHz, provided empirical RF-EMF data that defined the exposure conditions for this study. The measurements captured maximum exposure values from a 5G mmWave base station under different mobile usage scenarios (Voice Call, Video Call, and Video Streaming) in an outdoor environment. By applying these measured E-field strengths to the human body model, the simulations accurately reflect practical exposure conditions, allowing for a more realistic assessment of SAR and power density distributions. The recorded exposure values are detailed in Table 3.

TABLE 3. Maximum exposure RF-EMF values measured during different 30-minute tests [23].

Test	Maximum Exposure (V/m)
Voice call	4.50
Video call	5.27
Video streaming	5.71

The power supplied to the designed antenna was adjusted to match the measured E-field values from previous studies, ensuring consistency with real-world exposure. In the previous study, E-field measurements were taken over a 30-minute period for three mobile usage scenarios: voice call, video call, and video streaming, all operating at 29.5 GHz. These measured

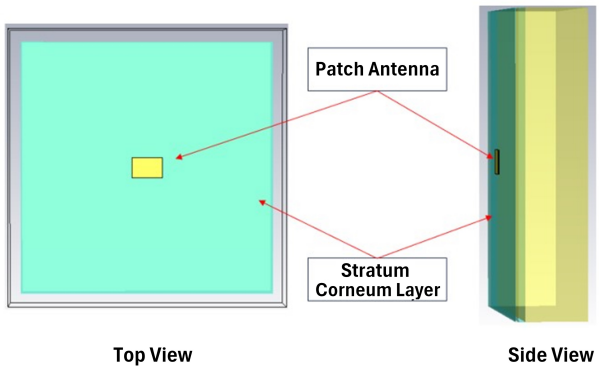

FIGURE 4. Antenna's location and orientation from the top view and side view.

values were then used in the simulation to investigate APD and PLD on a human skin model, providing insights into far-field RF-EMF exposure effects at millimeter-wave frequencies.

3. RESULTS AND DISCUSSION

In this study, the simulated results of APD were mapped, and its maximum value was identified for three applications, i.e., voice call, video call, and video streaming.

The simulated APD during the voice call application is shown in Figure 5. The directional arrows indicating the flow

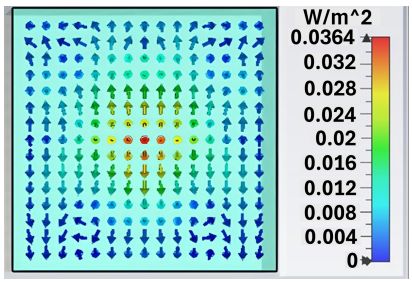

FIGURE 5. The APD during the voice call application.

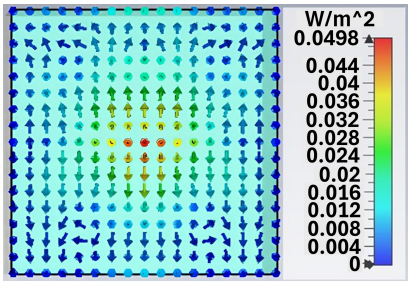

FIGURE 6. The APD during the video call application.

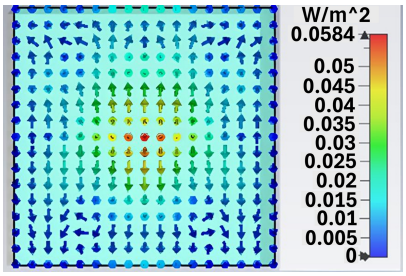

FIGURE 7. The APD during the video streaming application.

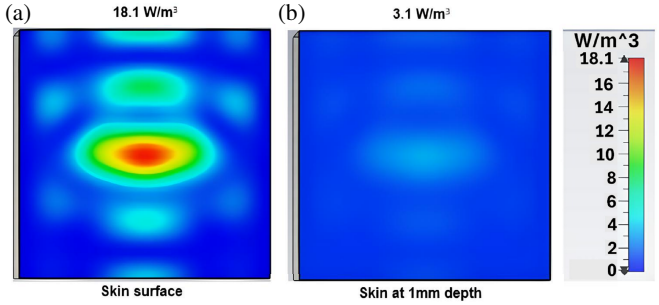

FIGURE 8. (a) PLD at the skin surface and (b) PLD at the skin depth of 1 mm for voice call application.

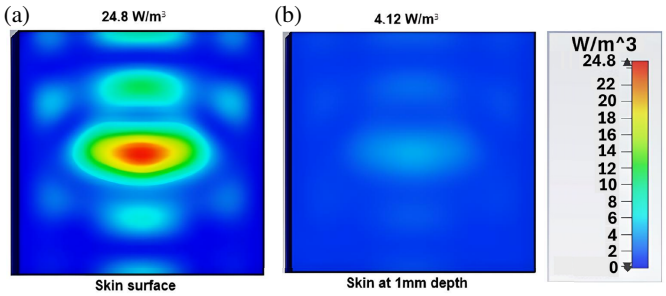

FIGURE 9. (a) PLD at the skin surface and (b) PLD at the skin depth of 1 mm for video call application.

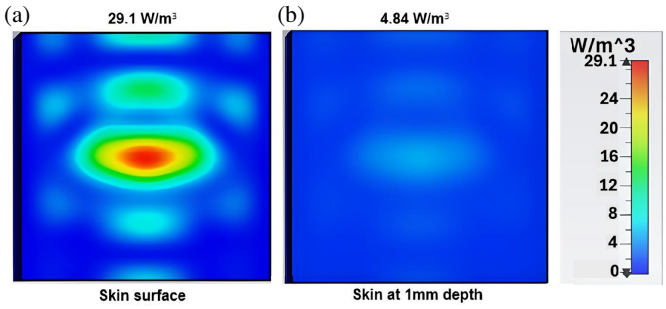

FIGURE 10. (a) PLD at the skin surface and (b) PLD at the skin depth of 1 mm for video streaming application.

of power distribution, with the highest intensity concentrated in the central region closest to the antenna, achieving the APD peak of 0.0364 W/m^2. This pattern follows the spatial distribution of the electromagnetic field, where the highest intensity is observed on the surface directly facing the antenna. As electromagnetic waves propagate outward, attenuation effects cause a gradual reduction in intensity.

Figure 6 shows the simulated APD for the video call application. Similarly, the highest intensity is concentrated near the antenna, with a peak of 0.0498 W/m^2. The decrease in intensity further away from the source is attributed to wave propagation and spatial distribution effects, where regions facing the antenna receive higher exposure than that further away.

As shown in Figure 7, the simulated APD for the video streaming application again shows the maximum intensity in the central region. The peak value is 0.0584 W/m^2. Since the antenna is centrally positioned within the skin sample, the highest intensity is localized on the surface directly facing it, while other areas experience reduced exposure due to the natural propagation and attenuation of electromagnetic waves.

Figure 8 presents the PLD for the voice call application, where the PLD was calculated as the ratio of absorbed power (W) to tissue volume (m^3). The highest observed PLD is 18.1 W/m^3 as shown in Figure 8(a). Meanwhile, Figure 8(b) shows a significant drop of maximum PLD to 3.1 W/m^3 at a depth of 1 mm.

Figure 9 illustrates the PLD for the video call application, with a peak at 24.8 W/m^3, as shown in Figure 9(a), thus having a notable decrease to 4.12 W/m^3 at a depth of 1 mm, as shown in Figure 9(b).

Figure 10 depicts the PLD for the video streaming application, where the maximum value reaches 29.1 W/m^3 as illustrated in Figure 10(a), dropping to 4.84 W/m^3 at a depth of 1 mm, as illustrated in Figure 10(b).

The simulation results indicate an upward trend in APD for voice calls (0.0364 W/m^2) to video calls (0.0498 W/m^2) by 31.09%. From video calls to video streaming (0.0584 W/m^2), the simulation results show increase by 15.90%. In addition, video streaming shows higher APD value than the APD values from voice call and video call, thus indicating the highest expo-

sure from video streaming. The simulation accuracy is within $\pm 0.02\,W/m^2$. Importantly, all APD values remain below the ICNIRP public exposure limit of $20\,W/m^2$ [34].

Similarly, the PLD shows an upward trend, with values of $18\,W/m^3$, $24\,W/m^3$, and $29\,W/m^3$ for voice calls, video calls, and video streaming, respectively, as shown in Figure 11. Namely, the PLD values from the skin surface decreased to values of $3.1\,W/m^3$, $4.1\,W/m^3$, and $4.8\,W/m^3$ for skin at 1 mm depth in cases of voice call, video call, and video streaming, respectively. This finding illustrates significant drops of exposure within mmWave frequency as it penetrates the skin.

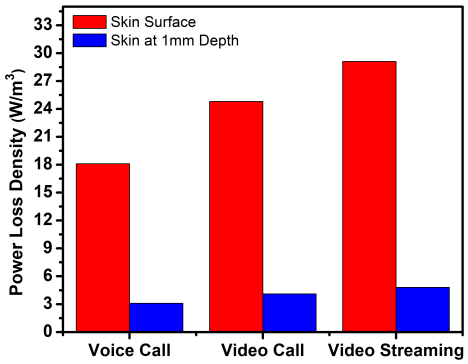

FIGURE 11. The PLD comparison at the skin surface and skin depth of 1 mm.

4. CONCLUSION

This study presents a pioneering effort in analyzing APD and PDL levels associated with 5G signals, particularly at mmWave frequencies (29.5 GHz) using a human skin model to analyze radiation effects under realistic application scenarios (voice call, video call, video streaming). Namely, using the real measurement results obtained during the operation of 5G mmWave BS in Cyberjaya, Malaysia as input data for the simulations conducted in CST software, we investigated APD and PLD values in this paper, which gave valuable insights about RF-EMF exposure. We meticulously designed the model of the transmitting antenna and adjusted its output power to generate the required E-field for various mobile applications. The results showed an increasing trend in APD across three applications, with maximum values of $0.0364\,W/m^2$ for voice calls, $0.0498\,W/m^2$ for video calls, and $0.0584\,W/m^2$ for video streaming. Importantly, the results are consistent with international safety standards (the obtained values remain significantly below the ICNIRP exposure limit of $20\,W/m^2$), providing reliable evidence of low exposure risks. The study also highlighted a substantial reduction in PLD at a depth of 1 mm inside the skin. However, continued research is essential for monitoring the long-term effects of RF-EMF exposure, particularly in densely populated areas with multiple BSs and varied usage patterns. Future studies should consider expanding the scope to include thermal effects on the skin and the cumulative impact of exposure over time. Also, comparing APD and PLD across different mmWave frequencies could be carried out. The ongoing research will contribute to a deeper understanding of the implications of 5G technology for public health.

ACKNOWLEDGEMENT

The paper is supported by Universiti Putra Malaysia (UPM) Geran Putra Berimpak (GBP/2023/9783500) and Ministry of Higher Education (MOHE) Fundamental Research Grant Scheme (FRGS/1/2021/TK0/UPM/01/1, File No. 03-01-21-2375FR. Vot No. 5540509).

REFERENCES

[1] Unit Perancang Ekonomi, Jabatan Perdana Menteri, "Dasar revolusi perindustrian keempat (4IR) negara," 2021.

[2] De la Fuente, A., R. P. Leal, and A. G. Armada, "New technologies and trends for next generation mobile broadcasting services," *IEEE Communications Magazine*, Vol. 54, No. 11, 217–223, 2016.

[3] Ancans, G., E. Stankevicius, V. Bobrovs, and N. Osis, "Analysis on interference impact of 4G/5G in 450 MHz on digital terrestrial television broadcasting," in *2019 Photonics & Electromagnetics Research Symposium — Fall (PIERS — Fall)*, 2173–2179, Xiamen, China, December 2019.

[4] Guo, Z., D. Chen, and Y. Yuan, "5G NR uplink coverage enhancement based on DMRS bundling and multi-slot transmission," in *2020 IEEE 20th International Conference on Communication Technology (ICCT)*, 482–486, Nanning, China, 2020.

[5] Song, Y.-J., S.-J. Lim, S.-K. Lee, and J.-S. Jang, "Adaptive digital beamforming for uplink coverage enhancement in 5G NR system," in *2019 27th Telecommunications Forum (TELFOR)*, 1–4, Belgrade, Serbia, 2019.

[6] Saha, R. K. and J. M. Cioffi, "Dynamic spectrum sharing for 5G NR and 4G LTE coexistence — A comprehensive review," *IEEE Open Journal of the Communications Society*, Vol. 5, 795–835, 2024.

[7] Dilli, R., "Analysis of 5G wireless systems in FR1 and FR2 frequency bands," in *2020 2nd International Conference on Innovative Mechanisms for Industry Applications (ICIMIA)*, 767–772, Bangalore, India, 2020.

[8] Bjornson, E., L. Van der Perre, S. Buzzi, and E. G. Larsson, "Massive MIMO in sub-6 GHz and mmWave: Physical, practical, and use-case differences," *IEEE Wireless Communications*, Vol. 26, No. 2, 100–108, 2019.

[9] Mallat, N. K., M. Ishtiaq, A. U. Rehman, and A. Iqbal, "Millimeter-wave in the face of 5G communication potential applications," *IETE Journal of Research*, Vol. 68, No. 4, 2522–2530, 2022.

[10] Kim, S., "Analysis of human exposure to electromagnetic fields in 5G uplink and downlink," *ArXiv Preprint ArXiv:2005.13295*, 2020.

[11] Simkó, M. and M.-O. Mattsson, "5G wireless communication and health effects — A pragmatic review based on available studies regarding 6 to 100 GHz," *International Journal of Environmental Research and Public Health*, Vol. 16, No. 18, 3406, 2019.

[12] Abdul-Al, M., A. S. I. Amar, I. Elfergani, R. Littlehales, N. O. Parchin, Y. Al-Yasir, C. H. See, D. Zhou, Z. Z. Abidin, M. Alibakhshikenari, *et al.*, "Wireless electromagnetic radiation assessment based on the Specific Absorption Rate (SAR): A review case study," *Electronics*, Vol. 11, No. 4, 511, 2022.

[13] Selmaoui, B. and Y. Touitou, "Association between mobile phone radiation exposure and the secretion of melatonin and cortisol, two markers of the circadian system: A review," *Bioelectromagnetics*, Vol. 42, No. 1, 5–17, 2021.

[14] Zou, Y., Q. Wang, Y. Chi, J. Wang, C. Lei, N. Zhou, and Q. Xia, "Electric load profile of 5G base station in distribution systems

based on data flow analysis," *IEEE Transactions on Smart Grid*, Vol. 13, No. 3, 2452–2466, 2022.

[15] Nasim, I. and S. Kim, "Mitigation of human EMF exposure in downlink of 5G," *Annals of Telecommunications*, Vol. 74, 45–52, 2019.

[16] Lagunas, E., C. G. Tsinos, S. K. Sharma, and S. Chatzinotas, "5G cellular and fixed satellite service spectrum coexistence in C-band," *IEEE Access*, Vol. 8, 72 078–72 094, 2020.

[17] Chataut, R. and R. Akl, "Massive MIMO systems for 5G and beyond networks — Overview, recent trends, challenges, and future research direction," *Sensors*, Vol. 20, No. 10, 2753, 2020.

[18] Prasad, K. N. R. S. V., E. Hossain, and V. K. Bhargava, "Energy efficiency in massive MIMO-based 5G networks: Opportunities and challenges," *IEEE Wireless Communications*, Vol. 24, No. 3, 86–94, 2017.

[19] Shafi, M., H. Tataria, A. F. Molisch, F. Tufvesson, and G. Tunnicliffe, "Real-time deployment aspects of C-band and millimeter-wave 5G-NR systems," in *ICC 2020 — 2020 IEEE International Conference on Communications (ICC)*, 1–7, Dublin, Ireland, 2020.

[20] Baki, A. K. M., "Beamwidth reduction of binomial array for 5G communications," in *2017 IEEE Region 10 Humanitarian Technology Conference (R10-HTC)*, 55–58, Dhaka, Bangladesh, 2017.

[21] Kim, S. and I. Nasim, "Human electromagnetic field exposure in 5G at 28 GHz," *IEEE Consumer Electronics Magazine*, Vol. 9, No. 6, 41–48, 2020.

[22] Moon, J.-H., "Health effects of electromagnetic fields on children," *Clinical and Experimental Pediatrics*, Vol. 63, No. 11, 422–428, 2020.

[23] Wali, S. Q., A. Sali, J. K. Allami, and A. F. Osman, "RF-EMF exposure measurement for 5G over mm-wave base station with MIMO antenna," *IEEE Access*, Vol. 10, 9048–9058, 2022.

[24] Christopher, B., S. M. Y, M. U. Khandaker, and P. J. Jojo, "Empirical study on specific absorption rate of head tissues due to induced heating of 4G cell phone radiation," *Radiation Physics and Chemistry*, Vol. 178, 108910, 2021.

[25] Tamim, A. M., M. R. I. Faruque, M. U. Khandaker, M. T. Islam, and D. A. Bradley, "Electromagnetic radiation reduction using novel metamaterial for cellular applications," *Radiation Physics and Chemistry*, Vol. 178, 108976, 2021.

[26] Christopher, B., Y. S. Mary, M. U. Khandaker, D. A. Bradley, M. T. Chew, and P. J. Jojo, "Effects of mobile phone radiation on certain hematological parameters," *Radiation Physics and Chemistry*, Vol. 166, 108443, 2020.

[27] Spandana, P. S. and P. V. Y. Jayasree, "Numerical computation of SAR in human head with transparent shields using transmission line method," *Progress In Electromagnetics Research M*, Vol. 105, 31–44, 2021.

[28] Psenakova, Z., J. Mydlova, and M. Benova, "Evaluation of Specific absorption rate in model of human head with Cochlear implant in different shielded spaces," in *2020 ELEKTRO*, 1–6, Taormina, Italy, 2020.

[29] Turgut, A. and B. K. Engiz, "Analyzing the SAR in human head tissues under different exposure scenarios," *Applied Sciences*, Vol. 13, No. 12, 6971, 2023.

[30] Karim, M. E. and A. B. M. A. Hossain, "SAR analysis of human head model using common antennas of 4G LTE mobile communications," in *2021 Fourth International Conference on Electrical, Computer and Communication Technologies (ICECCT)*, 1–5, Erode, India, 2021.

[31] Elabd, R. H. and A. J. A. Al-Gburi, "SAR assessment of miniaturized wideband MIMO antenna structure for millimeter wave 5G smartphones," *Microelectronic Engineering*, Vol. 282, 112098, 2023.

[32] Shrivastava, P. and T. R. Rao, "Specific absorption rate distributions of a tapered slot antenna at 60 GHz in personal wireless devices [wireless corner]," *IEEE Antennas and Propagation Magazine*, Vol. 59, No. 6, 140–146, 2017.

[33] Hamed, T. and M. Maqsood, "SAR calculation & temperature response of human body exposure to electromagnetic radiations at 28, 40 and 60 GHz mmWave frequencies," *Progress In Electromagnetics Research M*, Vol. 73, 47–59, 2018.

[34] International Commission on Non-Ionizing Radiation Protection (ICNIRP), "Guidelines for limiting exposure to electromagnetic fields (100 kHz to 300 GHz)," *Health Physics*, Vol. 118, No. 5, 483–524, 2020.

[35] Christ, A., T. Samaras, E. Neufeld, and N. Kuster, "Limitations of incident power density as a proxy for induced electromagnetic fields," *Bioelectromagnetics*, Vol. 41, No. 5, 348–359, 2020.

[36] Mahmoud, K. R., A. Baz, W. Alhakami, H. Alhakami, and A. M. Montaser, "The performance of circularly polarized phased subarray antennas for 5G laptop devices investigating the radiation effects," *Progress In Electromagnetics Research C*, Vol. 110, 267–283, 2021.

[37] Wu, T., T. S. Rappaport, and C. M. Collins, "The human body and millimeter-wave wireless communication systems: Interactions and implications," in *2015 IEEE International Conference on Communications (ICC)*, 2423–2429, London, UK, 2015.

[38] Romeo, S., O. Zeni, A. Sannino, S. Lagorio, M. Biffoni, and M. R. Scarfi, "Genotoxicity of radiofrequency electromagnetic fields: Protocol for a systematic review of in vitro studies," *Environment International*, Vol. 148, 106386, 2021.

[39] Pacchierotti, F., L. Ardoino, B. Benassi, C. Consales, E. Cordelli, P. Eleuteri, C. Marino, M. Sciortino, M. H. Brinkworth, G. Chen, *et al.*, "Effects of Radiofrequency Electromagnetic Field (RF-EMF) exposure on male fertility and pregnancy and birth outcomes: Protocols for a systematic review of experimental studies in non-human mammals and in human sperm exposed in vitro," *Environment International*, Vol. 157, 106806, 2021.

[40] Lagorio, S., M. Blettner, D. Baaken, M. Feychting, K. Karipidis, T. Loney, N. Orsini, M. Röösli, M. S. Paulo, and M. Elwood, "The effect of exposure to radiofrequency fields on cancer risk in the general and working population: A protocol for a systematic review of human observational studies," *Environment International*, Vol. 157, 106828, 2021.

[41] Lin, J. C., "Incongruities in recently revised radiofrequency exposure guidelines and standards," *Environmental Research*, Vol. 222, 115369, 2023.

[42] Korkmaz, E., S. Aerts, R. Coesoij, C. R. Bhatt, M. Velghe, L. Colussi, D. Land, N. Petroulakis, M. Spirito, and J. Bolte, "A comprehensive review of 5G NR RF-EMF exposure assessment technologies: Fundamentals, advancements, challenges, niches, and implications," *Environmental Research*, Vol. 260, 119524, 2024.

[43] Barnes, F. and B. Greenebaum, "Setting guidelines for electromagnetic exposures and research needs," *Bioelectromagnetics*, Vol. 41, No. 5, 392–397, 2020.

[44] Christ, A., T. Samaras, E. Neufeld, and N. Kuster, "RF-induced temperature increase in a stratified model of the skin for plane-wave exposure at 6–100 GHz," *Radiation Protection Dosimetry*, Vol. 188, No. 3, 350–360, 2020.

[45] Sellak, L., A. Khabba, S. Chabaa, S. Ibnyaich, A. Baddou, and A. Zeroual, "Miniaturized dual-band circular patch antenna design for 5G mmWave applications using ANFIS," in *2024 International Conference on Global Aeronautical Engineering and Satellite Technology (GAST)*, 1–6, Marrakesh, Morocco, 2024.

[46] Alblaihed, K. A., A. Abohmra, M. U. Rehman, Q. H. Abbasi, M. A. Imran, and L. Mohjazi, "Wideband series-fed patch antenna array with high gain and low sidelobe: Linearly and circularly polarized for 5G V2X applications," *IEEE Open Journal of Antennas and Propagation*, Vol. 5, No. 6, 1580–1591, 2024.

[47] Joshi, R. and A. Sharma, "Compact size and high gain microstrip patch antenna design for mmWave 5G wireless communication," in *2024 International Conference on Integrated Circuits and Communication Systems (ICICACS)*, 1–4, Raichur, India, 2024.

[48] Okwum, D., J. Abolarinwa, and O. Osanaiye, "A 30 GHz microstrip square patch antenna array for 5G network," in *2020 International Conference in Mathematics, Computer Engineering and Computer Science (ICMCECS)*, 1–5, Ayobo, Nigeria, 2020.